

Implication of cerebral circulation time in intracranial stenosis measured by digital subtraction angiography on cerebral blood flow estimation measured by arterial spin labeling

Kay Jann
Martinus Hauf
Frauke Kellner-Weldon
Marwan El-Koussy
Claus Kiefer
Andrea Federspiel
Gerhard Schroth

PURPOSE

Arterial spin labeling (ASL) magnetic resonance imaging to assess cerebral blood flow (CBF) is of increasing interest in basic research and in diagnostic applications, since ASL provides similar information to positron emission tomography about perfusion in vascular territories. However, in patients with steno-occlusive arterial disease (SOAD), CBF as measured by ASL might be underestimated due to delayed bolus arrival, and thus increased spin relaxation. We aimed to estimate the extent to which bolus arrival time (BAT) was delayed in patients with SOAD and whether this resulted in underestimation of CBF.

METHODS

BAT was measured using digital subtraction angiography (DSA) in ten patients with high-grade stenosis of the middle carotid artery (MCA). Regional CBF was assessed with pseudocontinuous ASL.

RESULTS

BATs were nonsignificantly prolonged in the stenotic hemisphere 4.1 ± 2.0 s compared with the healthy hemisphere 3.3 ± 0.9 s; however, there were substantial individual differences on the stenotic side. CBF in the anterior and posterior MCA territories were significantly reduced on the stenotic hemisphere. Severe stenosis was correlated with longer BAT and lower quantified CBF.

CONCLUSION

ASL-based perfusion measurement involves a race between the decay of the spins and the delivery of labeled blood to the region of interest. Special caution is needed when interpreting CBF values quantified in individuals with altered blood flow and delayed circulation times. However, from a clinician's point of view, an accentuation of hypoperfusion (even if caused by underestimation of CBF due to prolonged BATs) might be desirable since it indexes potentially harmful physiologic deficits.

The possibilities to study cerebral circulation with the simple and robust method of conventional angiography were recognized early by Edgar Moniz, the developer of cerebral angiography (1). Depending on the definitions of cerebral circulation, the period of time between contrast enhancement of the carotid syphon and the cerebral veins can range between 3 and 4 seconds (s) (2). By percutaneous puncture and direct injection of contrast into the carotid artery, Greitz (3) found a cerebral arteriovenous circulation time of 4 s in patients less than 40 years old compared to 4.2 s in older patients. Regional arteriovenous circulation time, defined as the time between maximum contrast filling of the carotid syphon to maximum filling of the regional veins was about 4 s in the frontal and between 4 and 5 s in the occipital lobes (4). Arterial circulation time is angiographically defined as the time between the start of opacification until complete washout of the contrast in the terminal arterial branches, which ranges between 1 s in the frontal and 1.5 s in the parietal lobes.

The interval between the end of the arterial filling and the beginning of the venous phase is angiographically defined as intermediate circulation time, or parenchymal phase, and varies from 0.25 to 1 s. With the recent improvements in biplane, flat panel digital subtraction angiography (DSA), the passage of the radiopaque contrast agent can be investigated with high resolution in space (200 μ m) and time (120 ms). It is now the commonly accepted gold standard in interventional neuroradiology for assessing vascular perfusion in stenosis which causes altered, prolonged, or even missing cerebral circulation.

Over the last decades, improvements in functional computed tomography (CT) and magnetic resonance imaging (MRI) enabled minimally invasive measurement of the cerebral circulation and brain perfusion with intravenous injection of iodine based x-ray or gado-

From the Department of Psychiatric Neurophysiology (K.J., ✉ jann@puk.unibe.ch, A.F.), University Hospital of Psychiatry and University of Bern; the University Institute of Diagnostic and Interventional Neuroradiology (M.H., F.K.W., M.E.K., C.K., G.S.), Inselspital and University of Bern, Bern, Switzerland.

Received 10 June 2015; revision requested 12 July 2015; last revision received 4 January 2016; accepted 30 January 2016.

Published online 13 July 2016.
DOI 10.5152/dir.2016.15204

linium-based contrast agents. Recent developments of arterial spin labeling (ASL), a completely noninvasive MRI technique, enable measuring and quantifying cerebral perfusion in terms of cerebral blood flow (CBF) using labeled blood itself as an endogenous contrast agent instead of x-ray or contrast agents, which must be injected intravenously for perfusion CT/MRI or even intra-arterially for conventional catheter angiography.

ASL has reached an increasing relevance in the characterization of physiologic and pathophysiologic cerebral processes in cerebrovascular diseases, degenerative disorders, psychiatric diseases, as well as in the field of basic neuroscience (5–9). The blood entering the brain through the carotid and the vertebral arteries is magnetically labeled in a tagging block during a given time period, which serves as an endogenous tracer. In more detail, the application of radiofrequency pulses to the hydrogen nucleus of the water molecules (actually the carrier of the “tagging information” together with the blood) changes its quantum physical energy state, from a most probable ground state to a state of elevated energy (10). However, there are some methodological and physiologic aspects that need to be considered when measuring and quantifying CBF using ASL measurements.

In whole brain ASL recordings, the blood is usually labeled on the level of the cervical internal carotid artery just below the base of the skull; therefore, one must account for the time the blood takes to reach the cortical capillary bed. This is achieved by introducing a post-label delay (PLD) between labeling and readout. However, the maximal possible PLD depends on the signal decay of the labeled spins (T1 decay) in brain tissue, thus it should be compatible

with the arterial transit times. In patients with a steno-occlusive arterial disease (SOAD), arterial transit times can be prolonged due to narrowing and obstruction of arteries and hence, blood flow. Since the introduction of ASL, studies have used this technique in SOAD with mixed success. On the one hand, bolus arrival time (BAT) delay effects have produced uncertainty about absolute CBF quantification, since it could lead to an underestimation of CBF (11). On the other hand, delay specific patterns have been pragmatically used to identify hemodynamically relevant stenosis (12). The narrowing of arteries in SOAD due to thickening of arterial walls or obstruction of an artery due to accumulation of plaques can impair blood flow and perfusion of brain parenchyma, causing steno-occlusive disease. This narrowing can affect the extracranial and internal carotid arteries, the vertebral arteries, and the intracranial arteries. Blood flow in SOAD can consequently be altered due to obstruction of the blood vessels. For ASL MRI in SOAD, an additional problem is that obstructed arteries can cause a delayed and dispersed bolus, resulting in uneven delivery of magnetically labeled blood to the parenchyma. Hence, labeled blood from obstructed arteries arrives in the readout plane later than that from an unaffected artery. With standard ASL sequences as provided by MRI scanner manufacturers, the readout is at a fixed time point after labeling (fixed PLD), and such sequences are sensitive to arterial transit time effects (13). Therefore, it is crucial to know whether the chosen PLD causes the readout to happen before the bolus of magnetically labeled blood arrives, because this could lead to underestimation of CBF that is superimposed on a possible true reduction of CBF. This problem can be partially addressed by using multi-delay readout ASL techniques that are less sensitive to transit time effects and thereby able to approximate true perfusion (14–16). However, multi-PLD techniques are not yet standard on MRI platforms. Nevertheless they provide valuable research tools to understand abnormal perfusion in steno-occlusive disease. Understanding the effect of delayed arrival times will facilitate the proper interpretation of ASL perfusion images in routine clinical imaging. Yun et al. (17) showed that in the case of intracranial stenosis, the correlation between CBF values from ASL and dynamic susceptibility contrast perfusion MRI weakens when transit times are slightly delayed, but not when extremely delayed. Chng et al. (18) assessed collateral flow with DSA

and territorial multi-PLD ASL and found that in at least a subset of patients with either intra- or extracranial stenosis, arrival of the delayed bolus via collaterals only yielded ASL signal for longer PLDs. This indicates a delayed but preserved CBF, which might be underestimated by single delay ASL. However, their work did not comment on absolute delay time and leaves to question the extent of BAT prolongation and whether CBF is underestimated.

Clinical recommendations for the treatment of SOAD vary according to the severity of the narrowing/obstruction, history of stroke, risk factors, and life expectancy for the patients; but in general these patients need to be treated when diagnosed. To gain insight into the value of standard ASL in the context of SOAD, the aim of the current investigation was twofold: 1) to estimate to what extent BAT (measured by DSA as gold standard for assessment of hemodynamic properties besides other contrast media-based perfusion measures) from labeling to the parenchymal phase of cerebral perfusion is delayed in patients with SOAD and 2) whether prolonged circulation times result in underestimation of CBF given the commonly applied PLDs.

Methods

Subjects

We included patients with symptomatic intracranial stenosis of the internal carotid artery (ICA) and/or the middle cerebral arteries (MCA), examined by DSA and ASL in the diagnostic workup of revascularization (endovascular or neurosurgical) therapy. Ten patients with SOAD (6 women, 4 men; mean age \pm standard deviation, 56 ± 12 years) met the inclusion criteria. Eight patients had unilateral stenosis; seven on the left side and one on the right side, while two patients harbored bilateral stenoses. Average grade of stenosis was $68.9\% \pm 12.3\%$. The study was approved by the local ethical committee, and all patients gave their written informed consent.

Pseudocontinuous arterial spin labeling

MRI was performed on a 3.0 Tesla (T) system (Magnetom TRIO, Siemens Medical). T1-, T2-, and diffusion-weighted imaging sequences were performed on a routine basis as well as time-of-flight and contrast-enhanced first pass gadolinium MRA of the head and neck vessels.

Pseudocontinuous ASL (pCASL) was used with the following parameters (19): 60 Hanning window-shaped radiofrequency pulses with duration 0.5 ms and

Main points

- Patients with a full or partial occlusion of carotid arteries may be assessed and clinically screened with noninvasive arterial spin labeling (ASL) MRI.
- However, there are some physiologic factors such as delayed bolus arrival times (BAT) in these patients that could lead to underestimation of cerebral blood flow (CBF).
- We found that severe stenosis was correlated with longer BAT and lower quantified CBF. Hence, CBF quantification models might require the option to integrate and correct for inter-individual differences in BAT.

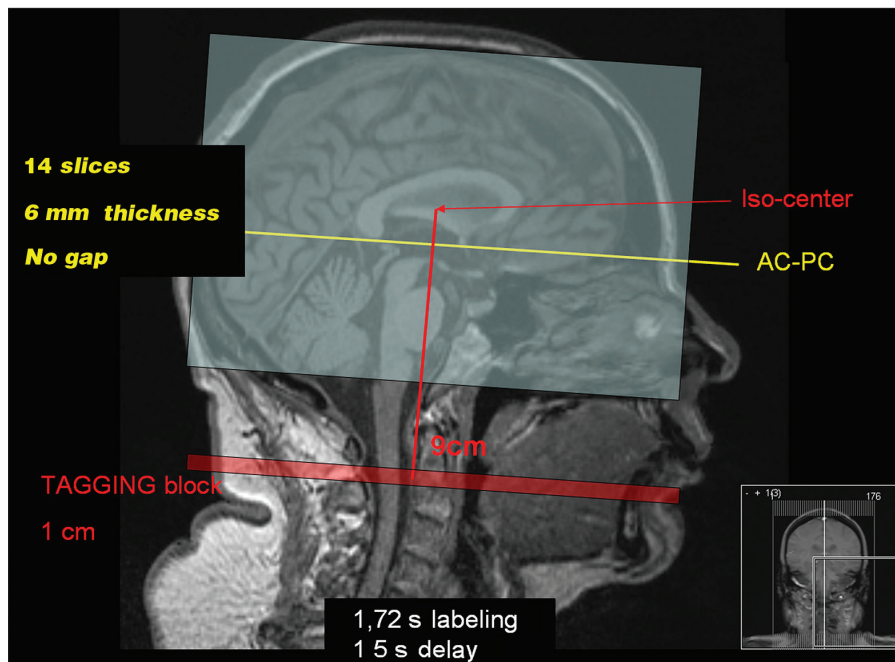


Figure 1. Arterial spin labeling recording setup and sequence parameters. AC, anterior commissure; PC, posterior commissure.

		Center of mass (MNI coordinates)		
		X	Y	Z
MCA anterior	Left	27.6	78.2	57.2
	Right	66.5	78.4	56.3
MCA posterior	Left	25.0	31.9	59.1
	Right	67.9	31.8	57.9

MNI, Montreal Neurological Institute; MCA, middle carotid arteries.

space between radiofrequency pulses of 0.9 ms; flip angle, 25°; slice-selective gradient, 6 mT/m; tagging duration (τ), 1720 ms; PLD, 1500 ms; and TR/TE, 4000 ms/13 ms 120 volumes. Fourteen axonal slices with 6 mm thickness were placed parallel to the anterior-posterior commissure line. The labeling block was 9 cm below the isocenter of the readout slices (Fig. 1). We used a pCASL sequence that should provide good signal-to-noise ratio (SNR) and reduced sensitivity to transit time effects when ΔT is sufficiently small with respect to T_1 of blood (allows for spin exchange with tissue water before spin decay) (19, 20). Image processing and CBF quantification were performed in SPM8 and with in-house written Matlab routines (MATLAB, The MathWorks, Inc.).

The raw images were first realigned to their mean to correct for motion distortions and co-registered to the individual anatomical scans. Secondly, we constructed a

flow-time series by simply subtracting the labeling images from the control images. This difference signal is proportional to CBF (21). The quantification to absolute CBF images was based on a single vascular compartment perfusion model as described below (22):

$$CBF = \left(\frac{\lambda \cdot \Delta M}{2 \cdot \alpha \cdot M_0 \cdot T_{1b}} \right) \cdot \left(\frac{1}{e^{-w/T_{1b}} - e^{-(\tau+w)/T_{1b}}} \right)$$

where the parameters were set as post-labeling delay (w)=1500 ms (adjusted for each slice), tagging duration τ =1720 ms, blood/tissue water partition coefficient λ = 0.9 [g/mL] and tagging efficiency α =0.85 (20). For 3.0 T, the decay time for labeled blood T_{1b} was assumed to be 1490 ms. M_0 are the equilibrium brain tissue magnetization images and were computed by averaging the control images (8, 23, 24).

Mean CBF images for the entire pCASL data-series were calculated. CBF and anatomical images were all normalized to the

normalized standard Montreal Neurological Institute (MNI) template (SPM8).

Finally, correlation analysis between the quantified CBF in the watershed areas of the MCA (defined with the WFUPickatlas in SPM (25), Table 1) and the rank-transformed BAT times was performed.

Digital subtraction angiography

Diagnostic DSA was performed on a biplane, flat panel angiographic system (Axiom Artis Zee, Siemens Medical). Details of the equipment, techniques and instruments have been described elsewhere (26). Briefly, four vessels cerebral DSA was performed in all patients by transfemoral approach. A nonionic iodinated contrast agent was injected through 5F catheter into both common carotid and at least the dominant vertebral artery. The passage of 8 mL contrast bolus through the carotid artery and its branches was imaged simultaneously in two planes by DSA in a time frame of 3–7 images per second. Complete DSA series, including the unenhanced mask images and late phase venous phase as well as the raw data were transferred and stored at the Picture Archiving and Communicating System, which enables image postprocessing, including remasking and motion correction for the retrospective re-evaluation of the data, to be performed by neuroradiologists with experience between five years and more than 20 years in diagnostic and interventional neuroangiography.

Cerebral flow parameters of the DSA series with normally up to 10 s duration (including 120 biplane images from the unenhanced mask to the late venous phase with 60 images in each plane) was performed retrospectively by analysis of the DSA images by the authors M.H., F.K., M.E., K.J., and G.S., who has more than 20 years of experience.

Corresponding to state of the art measurements by serial angiogram, BATs were estimated from a time point (TP-0) of proper opacification of the internal carotid artery just below the level of skull base (the level at which the ASL labeling block was placed), to different consecutive filling times of different vascular compartments for the healthy and stenotic hemispheres. The assessed time points for vascular compartments (Fig. 2) were the following: TP-0, 0 s: distal cervical segment of the internal carotid artery, just below the skull base and entering of the carotid artery into the bony carotid canal, corresponding to the labeling plane in ASL; TP-1: contrast opacification of the M1-M2 segments of the MCA; TP-2: appearance of small arteries; TP-3: disappearance of arteries and faint opacification of arterioles and

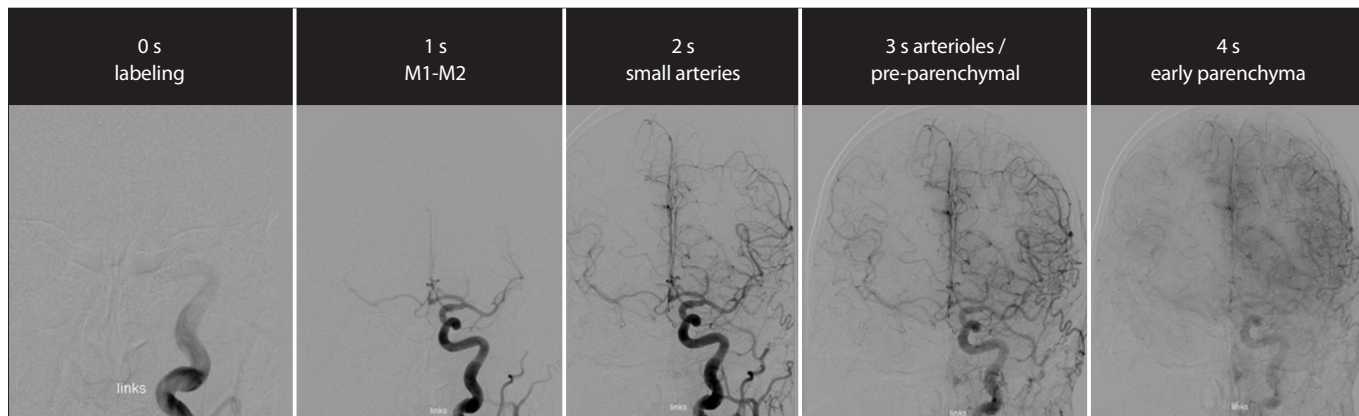


Figure 2. Approximated bolus arrival times from tagging plane to different vascular compartments demonstrated by digital subtraction angiography in a view following contrast injection into the left common carotid artery. Note the collateral flow to the contralateral hemisphere due to occlusion of the right internal carotid artery with a time delay of about 0.3 s only.

the preparenchymal phase; and TP-4: parenchymal phase, angiographically defined as diffuse contrast enhancement due to contrast in small vessels below the spatial resolution of DSA, resulting in an increase of x-ray attenuation of the pixel without direct outline of separate arteries or veins). Of special interest was the BAT calculated from the labeling plane TP-0 to the early parenchymal phase (TP-4) which was assumed to represent the time that labeled blood required at minimum to be considered as true perfusion in a physiologic sense. Furthermore, BAT differences for the healthy and stenotic hemispheres were calculated with regard to the severity of the occlusion.

Grading of stenosis was measured directly in millimeters, which is routinely implemented in the biplane modern angiography systems. In addition, relative values of stenosis were calculated: the minimal diameter of the stenosis was compared with the normal diameter proximally or distally from the stenosis and expressed as percentage of stenosis in accordance to NASCET criteria (27) and Schumacher et al. (28). These values, indicating the severity of stenosis were then non-parametrically correlated (Spearman's rank correlation) to the BAT times.

To further elucidate a potential difference between severity of stenosis and CBF and BAT, we divided the sample into patients with low-grade stenosis (<60%) and moderate to high-grade stenosis (>60%). We compared the CBF and BAT values of these subgroups using two-sample t-tests and within the subgroups between healthy and stenotic hemispheres using paired-sample t-tests.

Model fit to separate BAT effects and stenosis effects on CBF

In order to estimate the effect of stenosis on CBF while accounting for the BAT bias,

we computed a general linear model with individual CBF values for the anterior and posterior perfusion territories of the MCA, respectively, as dependent variables, and individual BATs from healthy and stenotic hemispheres as independent variables. We included an additional binary predictor into the model that coded for stenotic and healthy respectively (LS/H being logical 1 for stenotic and 0 for healthy).

$$CBF = \beta_0 + \beta_1 * BAT + \beta_2 * L_{S/H} + \epsilon$$

Under the assumption that only BAT affects CBF and stenosis does not cause true hypoperfusion, the beta-estimate for the binary predictor (β_2) should be zero, and non-zero otherwise (i.e., if stenosis causes a hypoperfusion). Significance of model fits was computed by an asymptotic chi-square statistic based on the deviance of the tested-models including a grouping variable for stenosis versus their reduced-models without the grouping variable.

For statistical analyses and tests we used the MATLAB Statistics Toolbox (The MathWorks, Inc.).

Results

BATs were slightly prolonged on the stenotic hemisphere (4.1 ± 2.0 s) compared with the healthy hemisphere (3.3 ± 0.9 s) but only with a statistical trend ($P_{(one-sided)} = 0.076$) (Table 2). However, in the two watershed areas of the MCA (MCA anterior and MCA posterior) the mean CBF images showed reduced values in the stenotic hemisphere (mean \pm standard deviation [SD] for MCA anterior 44.5 ± 15.9 mL/100 g/min and MCA posterior 42.4 ± 15.8 mL/100 g/min) compared with the healthy hemisphere (mean \pm SD for MCA anterior 51.8 ± 16.8 mL/100 g/min and MCA poste-

rior 51.7 ± 12.7 mL/100 g/min) (Fig. 3). Extracted CBF values for these two areas were significantly reduced ($P_{(one-sided)} = 0.050$ for MCA anterior and $P_{(one-sided)} = 0.036$ for MCA posterior). Correlations of CBF values with the estimated BAT to these areas as defined in the DSA images were significantly negative for MCA anterior ($P = 0.022$, $r = -0.51$, $R^2 = 0.26$; Fig. 4a) and MCA posterior ($P = 0.045$, $r = -0.45$, $R^2 = 0.20$; Fig. 4b). Moreover, the correlation analysis between the severity of the stenosis and the BAT revealed a significant positive correlation ($P = 0.020$, $r = 0.68$, $R^2 = 0.51$; Fig. 4c). Finally, under the assumption that CBF should be reduced with increasing stenosis, the correlation should be negative. We found a negative correlation in both watershed areas; however, the effect did not reach significance (MCA posterior $r = -0.54$, $P = 0.055$; MCA anterior $r = -0.29$, $P = 0.207$).

Thus, more severe stenosis was associated with longer BAT and lower quantified CBF. Moreover, Fig. 4c suggests that higher grades of stenosis resulted in a more pronounced prolongation of circulation times. The half-split subgroup analysis (beside the fact that the number of patients is small) revealed that BATs prolonged only in the group with moderate to high-grade (grade >60%) stenosis (mean BAT: healthy 3.48 s vs. stenotic 5.0 s, $P = 0.069$ [trend]), while for the low-grade group, BAT was similar on both hemispheres (mean BAT: healthy 3.2 s vs. stenotic 3.2 s, $P = 0.5$ [nonsignificant]). Furthermore, CBF in the MCA was significantly reduced for high-grade patients (MCA anterior $t = -2.15$, $P_{(one-sided)} = 0.049$; MCA posterior $t = -4.99$, $P_{(one-sided)} = 0.004$), while in the low-grade group CBF in the healthy and stenotic hemispheres were comparable (MCA anterior $t = -0.24$, $P = 0.411$; MCA posterior $t = 0.32$, $P = 0.381$).

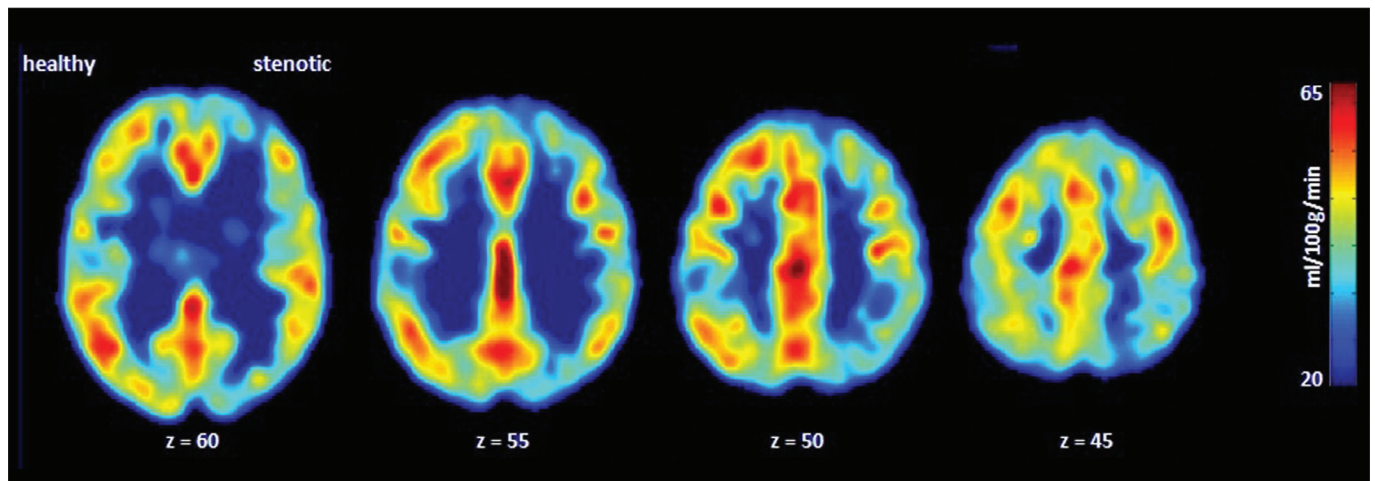


Figure 3. Mean cerebral blood flow (CBF) across the stenotic hemispheres (right side) and the healthy hemispheres (left side) of the nine patients. Reduced CBF in the watershed areas in the stenotic hemisphere can be observed.

Table 2. Patient characteristics including patient's age, side and grade of stenosis, estimated BATs for stenotic and healthy hemispheres, and visible collaterals

Patient No	Gender	Affected cerebral arteries	Grade (%)	Side	BAT (s) Stenotic	BAT (s) Healthy	Age (years)	Collaterals
1	M	ICA	60	Left	3.3	2.7	39	Left ACA by right A1
		ACOM	Hypoplastic	Left				
2	F	MCA/ICA	99	Left	5	3.3	73	Insufficient bypass
		PCOM	99	Left				
		PCA2	90	Left				
		ACOM	Hypoplastic	Right				
3	F	MCA1	60	Right	3	3	65	No collaterals
		ICA	40	Left				
4	F	MCA1	60	Left	2.7	2	63	No collaterals
5	M	MCA/ICA	60	Left	4	5	47	ACOM prominent (ACA1) PCOM hypoplastic
		MCA/ICA	50	Right	5			
6	M	MCA1	74	Left	9.3	4.7	49	Pial collaterals via ipsilateral ACA
		ICA	73	Left				
8	F	ACOM	Hypoplastic	Left	3.7	2.7	44	Vertical-MCA1
		PCOM	Prominent	Left				
9	F	MCA1	60	Left	3	3.3	48	No collaterals
10	M	ICA	70	Left	4	3.7	61	No collaterals

BAT, bolus arrival time; M, male; F, female; ICA, internal carotid artery; ACOM, anterior commissure of circle of willis; ACA, anterior carotid artery; MCA, middle carotid artery; PCOM, posterior commissure of circle of willis; PCA, posterior carotid artery.

Table 3. Generalized linear model fit parameters for anterior and posterior MCA territories

	Anterior MCA	Posterior MCA
β_0 (intersect)	61.30	63.25
β_1 (BAT effect)	-2.83	-3.45
β_2 (stenosis effect)	-5.21	-6.74

MCA, middle carotid artery; BAT, bolus arrival time.

Generalized linear models showed a moderate goodness-of-fit as calculated by pseudo- R^2 (0.12 and 0.25 for MCA anterior and MCA posterior, respectively). Significance of model fits were computed by comparing the tested models versus the reduced models and proved highly significant ($P = 1.802e-29$ and $P = 3.695e-48$ for MCA

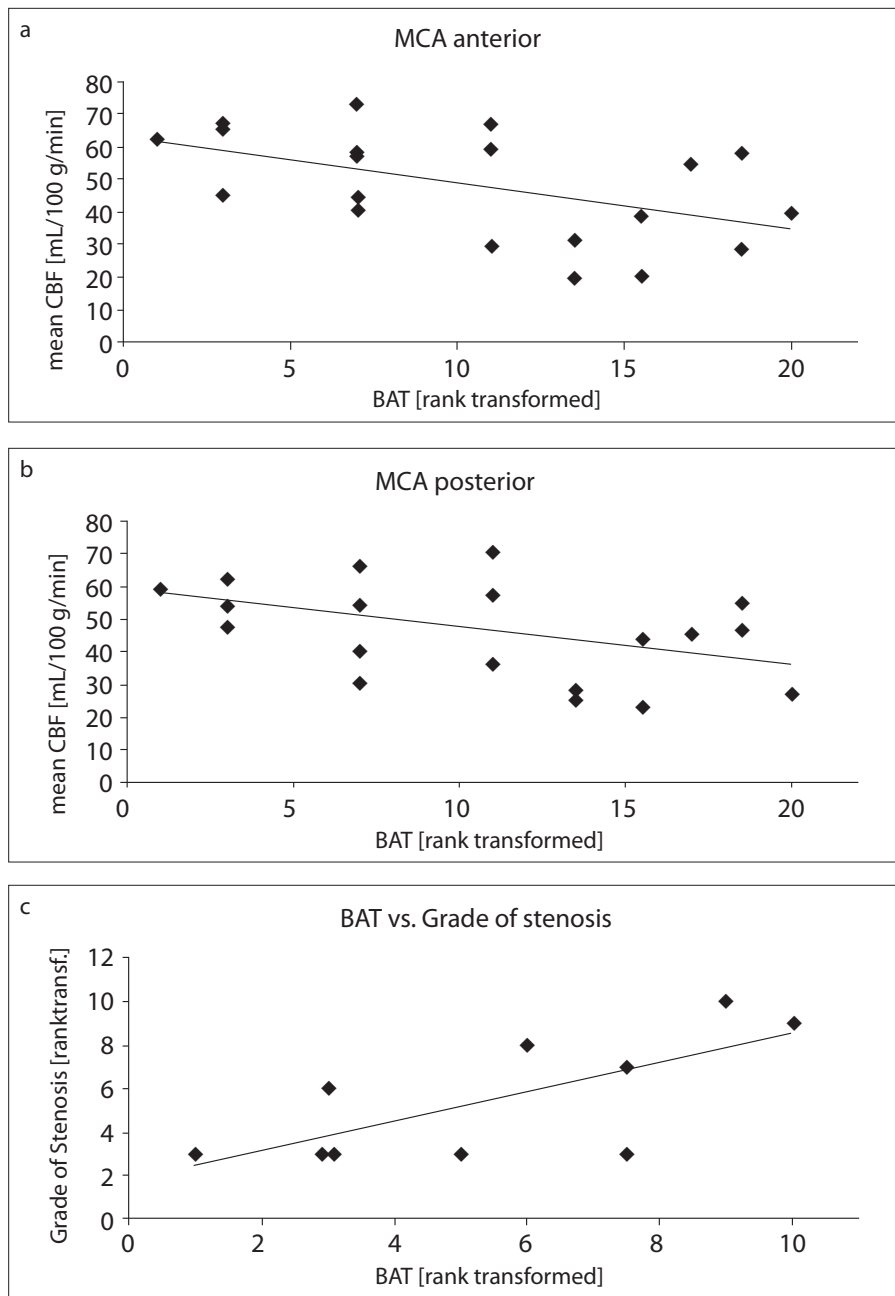


Figure 4. a–c. Correlation plots displaying the relation between the individual bolus arrival times (BATs; rank transformed) and the quantified CBF values in the anterior watershed area (a) and the posterior watershed area (b) of the middle carotid artery (MCA). Nonparametric correlation (c) displaying the relation between the individual BATs and the estimated grade of stenosis [%] according to NASCET criteria (27) and Schumacher et al. (28).

anterior and MCA posterior, respectively). Model estimation revealed that even when accounting for BAT, the stenotic hemisphere showed hypoperfusion of -5.21 mL/100 g/min in the anterior MCA territory and -6.74 mL/100 g/min in the posterior MCA territory. This shows that, for a similar BAT, CBF on the stenotic hemisphere was lower. Additionally, reduction of CBF due to BAT yielded a reduction of 2.83 mL/100 g/min for every second of delay in the anterior MCA territory and a -3.45 mL/100 g/min reduction for

every second of BAT in the posterior MCA territory (Table 3). Adjusting the CBF values for BAT in the healthy and stenotic territories according to the model fit parameters still provided a statistically significant difference between the hemispheres (MCA anterior: $t = -2.6220$, $P_{(one-sided)} = 0.014$; MCA posterior: $t = -3.10$, $P_{(one-sided)} = 0.006$).

Discussion

Our study showed that BATs were prolonged in the stenotic hemisphere 4.1 ± 2.0 s

compared with the healthy hemisphere 3.3 ± 0.9 s; however, there were substantial individual differences on the stenotic side. Along with prolonged BAT, CBF in the anterior and posterior MCA territories were significantly reduced on the stenotic hemisphere. This suggests that prolonged BAT causes underestimation of CBF in affected perfusion territories. Notably however, GLM modeling showed that for a similar BAT, CBF on the stenotic hemisphere still shows hypoperfusion. Finally, higher grade of stenosis was correlated with longer BAT and lower quantified CBF.

To quantify cerebral perfusion, positron emission tomography (PET) is regarded as the gold standard; however, it suffers from known limitations including limited availability, handling of radioactive substances, rather low spatial resolution, and high socioeconomic costs. Dynamic susceptibility contrast (DSC) MRI perfusion technique, a gadolinium-based technique, has several disadvantages including the fact that it only provides relative perfusion values, and it requires contrast injection, which is invasive and not without side effects, especially in patients suffering from renal diseases.

ASL emerged as an attractive, alternative noninvasive technique that uses the inflowing water spins in the artery as an endogenous contrast and provides quantitative measurements of CBF. The measure of blood flow per mass of tissue per minute is the established surrogate marker for the underlying metabolic processes. However, in physiology, brain perfusion is defined as the process of nutritive delivery to the brain tissue, which only takes place within the cortical capillaries (29). Accordingly, CBF measurements aim to represent the parenchymal phase of cerebral blood circulation.

Unfortunately, the commonly available ASL sequences have drawbacks related to the physical characteristics of the signal (spins and their relaxation) and the physiologic phenomenon (perfusion in capillary bed) they tend to assess. In healthy subjects, arterial transit times (to the level of Broca's knee) of 1600 ± 100 ms have been estimated using ASL (30). In the same study, tissue transit time, or the time that is needed to reach the capillary/tissue compartment, was calculated to be 1930 ± 110 ms. Other modalities, e.g., DSC-MRI and PET, found mean transit times to the cerebral cortex as 2.8 to 4.3 s (31). These values, as well as our results from conventional angiography, indicate that the optimal PLD for ASL measurements to capture spin exchange with tissue (true perfusion) is at the outer limit or beyond the time window of T1 decay where

most spins are still inverted and optimal SNR can be achieved.

This complicates measurements in patients with impaired blood flow dynamics or with cerebral vascular diseases. In patients with SOAD distal to the labeling plane (intracranial stenosis), the arrival times and tissue transit times are likely to be prolonged and dispersed.

In the current study, we aimed to estimate to what extent BAT, from labeling to the parenchymal phase of cerebral perfusion, is delayed in patients with SOAD, and whether prolonged circulation times result in underestimation of CBF given the commonly applied PLDs. This effect would result in an accentuation of CBF asymmetries in cases of high-grade stenosis. As reduced CBF is associated with impairments in cognitive functions due to chronic hypoperfusion, it is of interest to correctly detect such changes. Moreover, restoration of perfusion might lead to improved cognitive function after neurovascular therapy.

In the present study, we found reduced CBF in the flow territories of the anterior and posterior MCA of the stenotic hemisphere, while on the healthy hemisphere CBF was within normal range (32). In addition, we found prolonged cerebral circulation time due to the steno-occlusive disease and determined that this prolongation was associated with lower CBF values in the cortical regions of interest. In the healthy hemisphere, BAT to the parenchyma was around 3.3 s, while in the hemisphere with an intracranial stenosis, there was a nonsignificant prolongation (4.1 s). These values represent the transit delay between the ASL tagging block and the first readout slice (33), and are in line with the values reported in the literature for healthy subjects (2, 3). Moreover in patients with SOAD, increased timing parameters such as transit time and trailing edge time in the hemisphere ipsilateral to the occlusion were reported (5), and DSC-MRI revealed 1.75 s delay in bolus arrival and a dispersion of the bolus (34).

During this transition time, substantial T1 decay of the signal already occurs. Also, ASL quantification models (35) assume that inverted spins remain inverted until they have fully exchanged with tissue water at the region of interest (well mixed compartment) (10). This fit presumes that circulation times must be sufficiently short compared with the T1 relaxation of blood water. If the inverted spins relax before exchange with tissue water, then CBF is underestimated because fewer spins and subsequently reduced signal is measured within the cerebral cortex.

Another assumption is that the inverted spins in arteries do not contribute to the signal intensity change. The extraneous inverted spins can be accounted for by implementing crusher gradients in advanced ASL sequences that diminish the arterial signal by saturating blood in the vasculature (13, 36). Furthermore, insensitivity to arterial transit times can be achieved when the PLD is longer than the circulation time (13). But as our results demonstrate, the standard ASL single PLD as used in our study is not longer than the BAT. Usual delay times in ASL protocols are within 1 to 2 s. Together with the duration of the labeling (1.5 to 1.8 s), blood from different vascular compartments would be sampled. The leading edge of the bolus is already within the capillary bed (in our setting $1.5+1.72=3.22$ s) while the trailing edge of the bolus is still within the small arteries (1.5 s). However, T1 decay at 3.0 T is approximately 1.6 s, plenty of time for the blood in the capillary bed to almost fully relax and produce only very low SNR (37). The time-window of sufficient SNR for ASL acquisition, which is limited by the PLD and the associated T1 relaxation (38), is at the outer limit to sample signals from blood in the parenchymal phase with usual ASL recording parameters as used in this study. As a result, some assumptions of the ASL quantification models would be violated, and signal acquisition from blood in distinct vascular compartments and underestimation of quantified CBF values will hamper interpretation of ASL CBF maps.

The relation of BAT to quantified CBF in the watershed areas supports this observation (Fig. 3). The longer is the BAT, the lower is the CBF. This is a result that would be expected based on the quantification models when spins are not fully inverted once signal is sampled from the respective area. In cases with abnormally long BAT (>5 s) (39), a complete relaxation of the spins and thus zero CBF was assumed. However, collateral flow is rapid and can partly compensate for the delayed delivery of blood from the main feeding artery, resulting in detectable signal and preserved CBF in ASL. Another observation made by subgroup analysis in the present patient sample suggests that BAT was only delayed in patients with >60% stenosis, while lower grade of stenosis exhibited normal circulation time. Given this finding, we hypothesize that only moderate to high grade of stenosis produces decreased CBF. This could either be due to a real physiologic deficit or due to an underestimation of CBF caused by the delayed bolus arrival, or fewer tagged blood than assumed by the quantification model. To elucidate the con-

tributions of BAT and true hypoperfusion on the reduced CBF values, we computed a general linear model. The results confirmed that BAT caused a reduction of CBF in the watershed areas of the anterior and posterior MCA territories; although, this effect was in addition to a true physiologic hypoperfusion. After correcting CBF values for BAT effects, there was still a significant difference between the healthy and stenotic hemispheres. For these reasons, CBF values in SOAD are reduced on the affected hemispheres and can be overemphasized if BAT is prolonged.

This study demonstrates an inability to distinguish a real physiologic hypoperfusion from a possible ASL quantification model-based underestimation of CBF, if BATs are unknown. Nevertheless our results revealed the coupling of stenoses to delayed circulation times and reduced CBF values.

Since ASL has become part of the standard vendor packages for MRI systems, the possibility to noninvasively measure brain perfusion has gained interest with clinicians and researchers in different fields. However, knowledge of the underlying physiologic conditions and limitations of the ASL technique is crucial to the interpretation of results. This study may help to understand low CBF values on ASL maps in the context of SOAD. Furthermore, it demonstrates how to calculate post-label delay times in healthy subjects. From a clinician's point of view, an accentuation of hypoperfusion (even if caused by underestimation of CBF due to prolonged BATs) could be desirable since it indexes potentially harmful physiologic deficits. With this study, we wanted to address the problem of prolonged BATs in SOAD and how this affects the CBF values. This is an important caveat of standard single PLD ASL sequences that users in clinical settings need to be aware of. Our study demonstrates that reduced CBF represents physiologic hypoperfusion, but can be exaggerated due to underestimation caused by prolonged BAT. Even an underestimation of CBF due to BAT can highlight potential hemodynamically relevant stenosis, which can then prompt further follow-up with more invasive procedures. According to our findings, we believe that ASL has the potential to develop into a screening tool, since it is easily applicable, not very time consuming, and completely noninvasive. Also ASL screening might unveil an unknown SOAD when patients and subjects are examined for other clinical or research reasons. In addition, patients need to be followed after endovascular treatment to observe reversal

of hemodynamic abnormalities. ASL using endogenous contrast via spin labeling would be a very convenient method to evaluate the efficacy of the intervention in terms of restoration of CBF.

In conclusion, the measurement of perfusion using ASL remains a race between the decay of the spins and the delivery of labeled blood to the region of interest (33). Special caution is needed when interpreting CBF values quantified in individuals with altered blood flow and delayed circulation times. CBF quantification models might require integration and correction of inter-individual differences in BAT. In any case, ASL is suggested as a valuable tool for clinical assessment of SOAD patients as it emphasizes areas with altered perfusion and might even reflect the grade of stenosis.

Financial disclosure

This project is funded by grants from the Swiss National Foundation: Impact of quantitative MR perfusion imaging on the management of patients with carotid artery disease, 33CM30-124114. K.J., M.H., and F.K. were partially funded by this grant.

Acknowledgements

We thank Samantha J. Ma for proofreading and language editing of the manuscript.

Conflict of interest disclosure

The authors declared no conflicts of interest.

References

1. Moniz E. L'encéphalographie artérielle, son importance dans localisation des tumeurs cérébrales. *Revue Neurologique* 1927;72–90.
2. Moniz E. Sur la vitesse du sang dans l'organisme. *Annales de Medecine* 1932; 32:193–220.
3. Greitz T. A radiologic study of the brain circulation by rapid serial angiography of the carotid artery. *Acta Radiol Suppl* 1956; 140:1–123.
4. Leeds N, Taveras J. Dynamic factors in diagnosis of supratentorial brain tumors by cerebral angiography. Philadelphia: Saunders; 1969.
5. Bokkers RP, van Laar PJ, van de Ven KC, Kapelle LJ, Klijn CJ, Hendrikse J. Arterial spin-labeling MR imaging measurements of timing parameters in patients with a carotid artery occlusion. *AJNR Am J Neuroradiol* 2008; 29:1698–703. [CrossRef]
6. Hauf M, Wiest R, Nirkko A, Strozzi S, Federspiel A. Dissociation of epileptic and inflammatory activity in Rasmussen Encephalitis. *Epilepsy Res* 2009; 83:265–268. [CrossRef]
7. Horn H, Federspiel A, Wirth M, et al. Structural and metabolic changes in language areas linked to formal thought disorder. *Br J Psychiatry* 2009; 194:130–138. [CrossRef]
8. Jann K, Koenig T, Dierks T, Boesch C, Federspiel A. Association of individual resting state EEG alpha frequency and cerebral blood flow. *Neuroimage* 2010; 51:365–372. [CrossRef]
9. Walther S, Federspiel A, Horn H, et al. Resting state cerebral blood flow and objective motor activity reveal basal ganglia dysfunction in schizophrenia. *Psychiatry Res* 2011; 192:117–124. [CrossRef]
10. Detre JA, Leigh JS, Williams DS, Koretsky AP. Perfusion imaging. *Magn Reson Med* 1992; 23:37–45. [CrossRef]
11. Mutke MA, Madai VI, von Samson-Himmelstjerna FC, et al. Clinical evaluation of an arterial-spin-labeling product sequence in steno-occlusive disease of the brain. *PLoS One*. 2014; 9:e87143. [CrossRef]
12. Zaharchuk G, Do HM, Marks MP, Rosenberg J, Moseley ME, Steinberg GK. Arterial spin-labeling MRI can identify the presence and intensity of collateral perfusion in patients with moyamoya disease. *Stroke* 2011; 42:2485–2491. [CrossRef]
13. Alsop DC, Detre JA. Reduced transit-time sensitivity in noninvasive magnetic resonance imaging of human cerebral blood flow. *J Cereb Blood Flow Metab* 1996; 16:1236–1249. [CrossRef]
14. Johnston ME, Lu K, Maldjian JA, Jung Y. Multi-TI arterial spin labeling MRI with variable TR and bolus duration for cerebral blood flow and arterial transit time mapping. *IEEE Trans Med Imaging* 2015; 34:1392–1402. [CrossRef]
15. Kramme J, Gregori J, Diehl V, et al. Improving perfusion quantification in arterial spin labeling for delayed arrival times by using optimized acquisition schemes. *Z Med Phys* 2015; 25:221–229. [CrossRef]
16. Martin SZ, Madai VI, von Samson-Himmelstjerna FC, et al. 3D GRASE pulsed arterial spin labeling at multiple inflow times in patients with long arterial transit times: comparison with dynamic susceptibility-weighted contrast-enhanced MRI at 3 Tesla. *J Cereb Blood Flow Metab* 2015; 35:392–401. [CrossRef]
17. Yun TJ, Sohn CH, Han MH, et al. Effect of delayed transit time on arterial spin labeling: correlation with dynamic susceptibility contrast perfusion magnetic resonance in moyamoya disease. *Invest Radiol* 2013; 48:795–802. [CrossRef]
18. Chng SM, Petersen ET, Zimine I, Sitoh YY, Lim CC, Golay X. Territorial arterial spin labeling in the assessment of collateral circulation: comparison with digital subtraction angiography. *Stroke* 2008; 39:3248–3254. [CrossRef]
19. Dai W, Garcia D, de Bazelaire C, Alsop DC. Continuous flow-driven inversion for arterial spin labeling using pulsed radio frequency and gradient fields. *Magn Reson Med* 2008; 60:1488–1497. [CrossRef]
20. Wu WC, Fernandez-Seara M, Detre JA, Wehrli FW, Wang J. A theoretical and experimental investigation of the tagging efficiency of pseudocontinuous arterial spin labeling. *Magn Reson Med* 2007; 58:1020–1027. [CrossRef]
21. Luh WM, Wong EC, Bandettini PA, Hyde JS. QUIPSS II with thin-slice T1 periodic saturation: a method for improving accuracy of quantitative perfusion imaging using pulsed arterial spin labeling. *Magn Reson Med* 1999; 41:1246–1254. [CrossRef]
22. Alsop DC, Detre JA, Golay X, et al. Recommended implementation of arterial spin-labeled perfusion MRI for clinical applications: A consensus of the ISMRM perfusion study group and the European consortium for ASL in dementia. *Magn Reson Med* 2015; 73:102–116. [CrossRef]
23. Kilroy E, Apostolova L, Liu C, Yan L, Ringman J, Wang DJ. Reliability of two-dimensional and three-dimensional pseudo-continuous arterial spin labeling perfusion MRI in elderly populations: Comparison with 15o-water positron emission tomography. *J Magn Reson Imaging* 2014; 39:931–939. [CrossRef]
24. Wang J, Aguirre GK, Kimberg DY, Roc AC, Li L, Detre JA. Arterial spin labeling perfusion fMRI with very low task frequency. *Magn Reson Med* 2003; 49:796–802. [CrossRef]
25. Maldjian JA, Laurienti PJ, Kraft RA, Burdette JH. An automated method for neuroanatomic and cytoarchitectonic atlas-based interrogation of fMRI data sets. *Neuroimage* 2003; 19:1233–1239. [CrossRef]
26. Mordasini P, El-Koussy M, Schroth G, Brekenfeld C, Beck J, Gralla M. Applicability of tableside flat-panel detector CT parenchymal cerebral blood volume measurement in neurovascular interventions: Preliminary clinical experience. *AJNR Am J Neuroradiol* 2012; 33:154–158. [CrossRef]
27. Beneficial effect of carotid endarterectomy in symptomatic patients with high-grade carotid stenosis. North American Symptomatic Carotid Endarterectomy Trial Collaborators. *N Engl J Med* 1991; 325:445–453. [CrossRef]
28. Schumacher HC, Meyers PM, Higashida RT, et al. Reporting standards for angioplasty and stent-assisted angioplasty for intracranial atherosclerosis. *Stroke* 2009; 40:e348–365. [CrossRef]
29. Wang J, Alsop DC, Song HK, et al. Arterial transit time imaging with flow encoding arterial spin tagging (FEAST). *Magn Reson Med* 2003; 50:599–607. [CrossRef]
30. Mildner T, Moller HE, Driesel W, Norris DG, Trampel R. Continuous arterial spin labeling at the human common carotid artery: the influence of transit times. *NMR Biomed* 2005; 18:19–23. [CrossRef]
31. Ibaraki M, Ito H, Shimosegawa E, et al. Cerebral vascular mean transit time in healthy humans: a comparative study with PET and dynamic susceptibility contrast-enhanced MRI. *J Cereb Blood Flow Metab* 2007; 27: 404–413. [CrossRef]
32. Ingvar DH, Cronqvist S, Ekberg R, Risberg J, Hoedt-Rasmussen K. Normal values of regional cerebral blood flow in man, including flow and weight estimates of gray and white matter. A preliminary summary. *Acta Neurol Scand Suppl* 1965; 14:72–78.
33. Wong EC. Quantifying CBF with pulsed ASL: technical and pulse sequence factors. *J Magn Reson Imaging* 2005; 22:727–731. [CrossRef]
34. Calamante F, Gadian DG, Connelly A. Quantification of perfusion using bolus tracking magnetic resonance imaging in stroke: assumptions, limitations, and potential implications for clinical use. *Stroke* 2002; 33:1146–1151. [CrossRef]
35. Williams DS, Detre JA, Leigh JS, Koretsky AP. Magnetic resonance imaging of perfusion using spin inversion of arterial water. *PNAS* 1992; 89:212–216. [CrossRef]
36. Wong EC, Buxton RB, Frank LR. Quantitative imaging of perfusion using a single subtraction (QUIPSS and QUIPSS II). *Magn Reson Med* 1998; 39:702–708. [CrossRef]
37. Lu H, Clingman C, Golay X, van Zijl PC. Determining the longitudinal relaxation time (T1) of blood at 3.0 Tesla. *Magn Reson Med* 2004; 52:679–682. [CrossRef]
38. Detre JA, Wang J. Technical aspects and utility of fMRI using BOLD and ASL. *Clin Neurophysiol* 2002; 113:621–634. [CrossRef]
39. Olivot JM, Mlynash M, Zaharchuk G, et al. Perfusion MRI (Tmax and MTT) correlation with xenon CT cerebral blood flow in stroke patients. *Neurology* 2009; 72:1140–1145. [CrossRef]